THE EFFECTS OF PRE-ALLOYED STEELS POWDER COMPOSITIONS ON BUILD QUALITY IN DIRECT METAL LASER RE-MELTING.

SP Akhtar, CS Wright and M Youseffi

Engineering Materials Research Group, University of Bradford, Bradford, UK

Abstract

This paper describes recent studies investigating the relationships between alloy composition and processability of a range of pre-alloyed stainless and tool steel powders melted using CO_2 and Nd:YAG lasers. Factors considered in this paper that influence processability are particle size and shape, particle distribution, fluidity, wetting, and scan conditions. However, thermodynamic modelling, validated by experiment, suggests that alloy composition is a significant factor affecting processability. A short solidification range corresponds to a significant increase in build quality.

Introduction

Selective laser sintering (SLS) is one of the more important solid freeform manufacturing processes developed in the last 10-15 years [1]. One of the main applications of SLS is for the manufacture of prototype or low volume production tooling using steel powders. Commercial systems are available which generate parts from either polymer coated steel powders [DTM Rapid Tool 2.0^{TM}] or by processing a mixture of metal powders that contains a low melting point component [EOS Direct Tool ^{TM}]. The need to post process, i.e. infiltrate with bronze, or the reliance on a low melting point liquid, leads to components with poor mechanical and tribolological properties. This has led to a number of studies aimed at investigating Direct Metal Laser Re-melting (DMLR) pre-alloyed metal powders with the aim of eliminating the above disadvantages. These studies generally made use of commercially available powder stainless steel [2, 3], and tool steels [4 - 6]. Stainless Steel powders have been DMLR processed to give multi-layer samples with densities of +99% [3] compared with only 60% for HSS [6]. This paper presents some results of ongoing investigations into the melting / densification behaviour of pre-alloyed metal powders during DMLR which has the ultimate aim of identifying the factors which control the ability to fabricate fully dense, multi-layer components.

Experimental Procedure

Five types of powder were used in this investigation. Annealed water atomised M2 (WA-M2), gas atomised M2 (GA-M2), gas atomised H13 (GA-H13) with varying contents of carbon and water atomised P58 (WA-P58), an experimental high speed steel (Fe-14Mo-4Cr-14C) . The water atomised M2 was sourced from Powdrex, UK and the gas atomised powders were obtained from Osprey Metals Ltd, UK. Water atomised powders were sieved in compliance with ASTM standard E11 to give the following size fractions; >75-150μm, >38-75μm and <38μm for water atomised powders. Identical size fractions were obtained for gas atomised powders from the suppliers.

Direct metal laser re-melting studies were performed on specially constructed machines at the Universities of Leeds and Liverpool. The Leeds machine includes a 250W continuous wave (CW) CO_2 laser. Initial studies were conducted at a beam size of 1.1mm diameter. This was subsequently reduced to 0.55mm diameter. Sintering was performed in an

141

argon shroud. Details of this machine are given in Reference [2]. The Liverpool system, described by Morgan, et. al. [3], consisted of a Rofin Sinar 90W, flash lamp pumped Q-Switched Nd : YAG laser. An analogue galvanometer-scanning head attains beam position over an area of 80 x 80 mm2. Pulse repletion rates were in the range 0 – 60kHz and minimum beam diameter is 80μm. The shroud gas was nitrogen.

The two systems employed different approaches to placing layers of powder. In the Leeds machine, the initial powder layer comprised loose powder to a depth of 5 mm contained in a mild steel tray. This layer was levelled with a blade to ensure a flat powder surface. Subsequent layers were deposited using a hopper system. The layer depth was 0.4 mm. In the Liverpool machine mild steel sheet was used as a substrate. In this system, the powder delivery system was optimised for an even 100μm coating of powder to be layered for every build layer [3]. Whilst all size fractions studied could be processed on the Leeds machine, the Liverpool machine was restricted to processing just the <38μm fraction.

After sintering samples were prepared for metallographic examination by mounting and grinding on SiC paper to 1200 grit, then polished on cloths impregnated with 6 and 1μm diamond. Polishing was completed using 0.05μm γ-alumina. Samples were studied in the etched and un-etched conditions. Samples were etched in 5 or 10% Nital. Samples were examined using both optical and scanning electron microscopy techniques.

Isopleths were calculated for the M2, H13,316L, P58 systems using ThermoCalc[TM] [www.thermocalc.se] software and the SGTE SSOL database in order to understand the correlation between alloy composition, solidification ranges and processability.

Results and Discussions.

Powders.
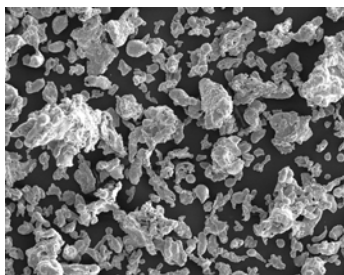Typical SEM micrographs for the different powders are given in Figures 1 and 2.

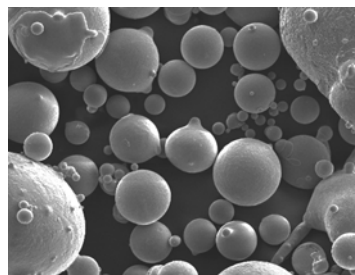Fig1 . M2 water atomised HSS powder. As received <150μm. SEM X150, 20KV

Fig 2. P58 gas atomised HSS powder, As received. SEM X1000, 20KV

The water-atomised powders were composed of highly irregular particles and, as such, are typical of this method of powder production. As expected the gas-atomised powders were composed of spherical particles. However, whilst the <38μm GA-P58 size fraction consisted of spherical particles with smooth surfaces the particle surfaces of the coarser fractions were much rougher due to the presence of many smaller satellites formed as a result of collisions during atomisation, Figure 2. The effects of powder size and morphology on DMLR are discussed later. The various size fractions used, along with Apparent Density and flowability (Hall Flowmeter) data are given in Tables 1 and 2.

142

Table 1 Powder properties for WA-M2 HSS and WA-P58 powder.

Powder Fraction (μm)	WA-M2 HSS powder Flow rate (s/50g)	WA-M2 HSS powder Apparent Density (g/cm^3)	WA-P58 Apparent Density (g/cm^3)	WA-P58 Hall Flow rate (s/ 50g)
-150	52.1	2.27	2.70	No flow
+75/-150	55.4	2.14	2.20	51.3
+38/-75	59.8	2.18	2.52	No flow
-38	No flow	2.60	2.87	No flow

Table 2 Powder properties for GA-M2 HSS and GA-P58 powder

Powder Fraction (μm)	Apparent Density (g/cm^3)	Hall Flow rate (s/ 50g)
GA-P58 (As-Received –150)	5.00	18.2
GA-M2 -75/+150	3.97	23.7
GA-M2 -38	4.31	No flow

At the outset of this work two methods were envisaged for the manufacture of high density, multi-layer components as discussed in previous work [7]. The preliminary strategy was to partially melt successive powder layers together followed by a post processing step. The second method was to completely re-melt the powder layers. In order to identify appropriate processing conditions for the two processing strategies, the heating and melting behaviour of each batch of powder was systematically studied using the CO_2 laser SLS machine at Leeds. Single tracks were produced for a wide range of Laser power and scanning conditions.

Process Maps. Single track process maps were produced using the CW CO_2 DMLR machine for M2, H13 and P58. The process maps detail the heating and melting behaviour of the metal powders as scan speed and laser power change. These highlight regions where the melt pool remained continuous, i.e. did not fragment or ball. A fragmented melt pool has been shown to reduce the surface quality and density of layers [8]. Typical Process Maps for M2 and H13 powders are given Figure 3 . The maps show several qualitative regions: continuous flattened tracks, continuous rounded tracks, melted and balled tracks, partially melted and unmelted regions.
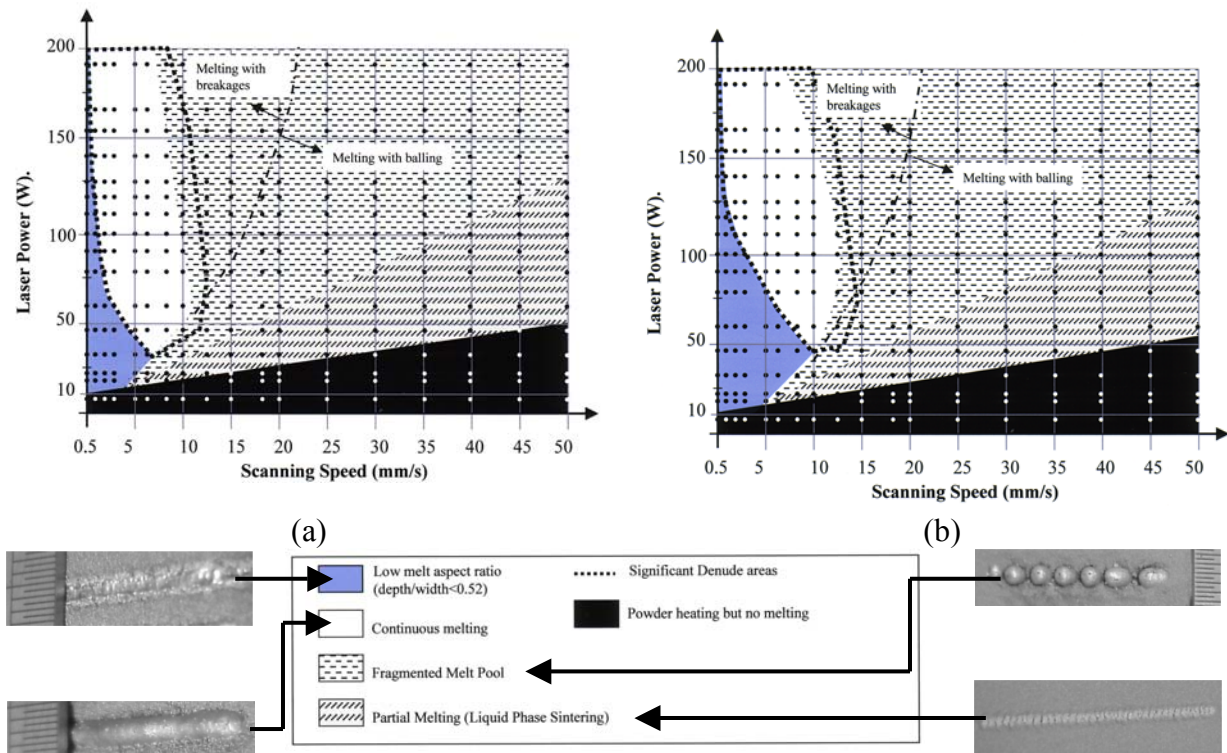
Figure 3.   CW CO_2 laser process maps for (a) gas-atomised M2 <150/+75μm
fraction 1.1mm spot size (b) gas-atomised H13 <150/+75 μm fraction,
0.6mm spot size

A feature of these process maps for single track scanning of M2 and H13 powders was that the size of the regimes and the positions of the boundaries defining each regime were comparable, irrespective of alloy composition, or whether or not the powder was gas or water atomised, or processing with spot sizes of 1.1 or 0.6mm diameter, or even size fraction used, e.g. Figures 3(a) and (b). Moreover, the maps were comparable to ones reported elsewhere for 314HC stainless steel [8] and Fe-14Mo-4Cr-1.4C [9] experimental HSS alloys.

In order to fabricate multi-layer blocks (12 x 12 x 12 mm³), experiments were performed on the CO_2 laser SLS machine using conditions within both the partial melting and continuous melting regimes. However, the sub 38μm water and gas atomised size fractions were difficult to spread due to their poor flowability, layers tended to form furrows. Work with these powders was, therefore, discontinued. With the coarser fractions, irrespective of powder type or particle sizes, processing within the partial melting regime was unsuccessful because insufficient melting took place to bond the next layer on to the previous layer, making it impossible to build intact blocks [10]. Thus it was not possible to investigate fabrication of multi-layer components for M2 via the partial melting-post processing route. Gas atomised M2 multi-layer blocks fabricated from 25 individual powder layers were produced using conditions within the continuous melting regime. The resultant blocks were very porous and had very rough surfaces. Typical micrographs consisted of M_2C and M_6C eutectics dispersed in a martensitic matrix and a definite interfacial feature was also present between bonded layers comprising eutectic carbide structures [7].

On processing the +75/-150μm H13 size fraction in the CW CO_2 system it was noted that for scan conditions in the low melt aspect ratio regime, Figure 3 (b), produced tracks that

144

were 30-40% flatter than for M2 powders. So from a build point of view H13 had better processability in the CW CO_2 laser system but again multi-layer blocks produced from H13 powders were very porous and fragile, and only a maximum density of 70% was obtained. As with M2, processing H13 powders in the partial melting regime was unsuccessful since it was not possible to bond the melted layer to the underlying layer.

Much more promising results were obtained with the Nd : YAG DMLR machine. This system employed much higher scan speeds and a layer thickness of 0.1mm. In the Nd : YAG system no systematic process maps were collated. Conditions were selected based on processing parameters used to produce high density multi-layer blocks from 316L powders [3]. Water atomised M2 powders were processed at scan speeds of 10 –500mms⁻¹, laser current 16-20A, Spot size = 0.1 mm, Beam overlap of 25-80%, pulse repetition frequency of 0kHz, layer thickness 100μm. Both single and 3 layer samples were produced but the scanned areas contained large amounts of un-melted powder. Removal of this by ultrasonic cleaning revealed that the beds were very porous. The porosity levels were unaffected by scanning conditions. This high level of porosity was attributed to the low apparent density of the water atomised powder (Table 1) arising from its highly irregular shape.

Further experiments with WA and GA M2 powders were carried out at layer thicknesses of 100 and 50μm, pulse repetition frequencies of 40 and 50kHz, scan speed = 500 mms⁻¹, current = 20A, spot size = 100μm, beam overlap = 50%. Blocks 5 x 15 x 15mm³ were produced. Operating in pulse repetition mode resulted in an increase in density compared to continuous mode. However resultant densities, which were the highest attained in this study on laser scanning of M2 powders, were only 5.5 gcm⁻³, i.e. ~67% relative, Figure (a). Despite the higher apparent density of the <38μm gas atomised powder, Table 2, use of this powder had no beneficial effects on the density of laser scanned blocks, densities were similar to those obtained for <38μm water atomised M2 powder. So it would appear that in pulsed mode final density is independent of initial powder bed density. Also for the range of conditions studied it would appear that density is unaffected by pulse frequency.
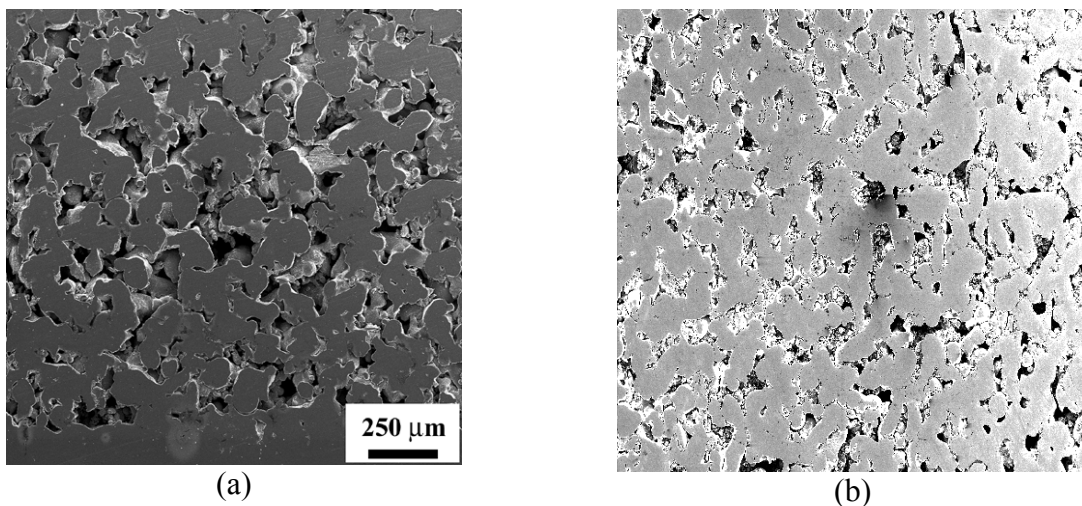

(a)   (b)

Figure 4.   Micrographs of Nd : YAG laser scanned multi-layer (a) GA-M2, 500 mms⁻¹scan speed, 50% beam overlap, current 20A, spot size 0.1mm, pulse rate 40kHz. (100μm layer thickness). (b) GA-H13 <22μm. Scan speed = 500mms⁻¹, beam overlap = 50%, laser current = 20A, spot = 0.1mm, pulse rate 30kHz.

Our work indicates that since the maximum density for M2 was only 60% relative, and 67% relative using CW CO_2 and Nd : YAG systems, respectively this is not a suitable alloy for processing by DMLR. Moreover the microstructures produced contained detrimental microstructural features such as carbide clusters and thermal cracking [7]. Consequently, even if M2 powders could be processed to ~100% density by DMLR, such regions would also be potential points of weakness. Carbide clusters are preferred sites for crack nucleation and propagation at low applied stresses under static and dynamic loading [11]. Given that solidification behaviour of individual HSS compositions are all similar, it is very likely that similar features would occur with other types of HSS processed by DMLR, suggesting that HSSs are unsuitable for processing by this fabrication route.

However, processing GA-H13 at conditions of pulse repetition frequency of 30kHz gave well-bonded, multi-layer blocks with a density of 85-90% Fig 4(b). Processing under these conditions takes place within the melting with balling region of Figure 3 (b), giving a sample structure somewhat different from that achieved in the CW CO_2 laser. The microstructure comprised martensitic cellular grains. Grain boundaries were delineated by continuous carbide network and the matrix was martensitic. The microstructure of Nd : YAG processed material was finer than the CW CO_2 processed H13. The finer microstructure is indicative of a faster cooling rate . However, thermal cracking was also present in these samples [14].

In the Nd:YAG system further experiments were carried out, in which additional carbon was added to H13 powders [12]. It was thought that a reduction in the melting point would be considered advantageous when the material was laser sintered and hence aid the ease of processability. However it was found that as carbon is added to H13, the increased carbon content lead to severe balling of the molten metal and caused a lack of wetting with the resulting material became increasingly porous. Thus, it appears that the higher carbon levels are detrimental to the DMLR processing of tool steels, as carbon appears to reduce the flow of the melt as it wets the underlying material. Higher carbon contents also increased the surface roughness [12].

Given that the powder properties (flowability, AD and morphology) of gas atomised M2 and H13 used in these studies were comparable, this would suggest that other factors have a very important role in determining the densification behaviour during the laser scanning of powders. In previous studies factors considered important on processing powder via DLMR include particle size, shape, distribution, melt viscosity, wetability, surface tension, oxide stability [3] and powder oxygen content [4,5]. For example, from the results of single scan studies Nui and Chang [4, 5] considered the high oxygen content of water atomised M2 powder compared to gas atomised M2 to be detrimental to their processability. The results presented in the current paper suggest that alloy composition is also an important factor in determining whether high density can be achieved. This is particular so with the Nd:YAG system where it has been possible to process similar sized stainless steel powders, <22μm, to 100% density [3].

In conventional supersolidus liquid phase sintering (SLPS) of pre-alloyed powders a critical factor for determining processability is the melting-freezing range since a wide range correlates to a wide process window 16. Wright et. al. [17] have used German's model of supersolidus liquid phase sintering [16], in conjunction with computer-aided alloy, to design tool steel compositions with enhanced sinterability [17]. The P58 composition was one such composition [17].

146

In the case of DMLR, processing generally involves solidification of a fully molten bead rather than partially melted powders as in case of conventional SLPS. An important factor in conventional casting is melt fluidity [18]. Melt fluidity determines the ease at which a molten alloy will fill a complex cavity. High melt fluidity is an essential requirement for a casting alloy since this facilitates the production of complex castings. High fluidities are associated with eutectic alloy compositions whereas long freezing range alloys exhibit low fluidities [18]. In the case of DMLR processing, alloy fluidity is likely to have an influence on the way in which the melt bead interacts with surrounding powder and the morphology of the resultant track as the bead solidifies.

The results from thermodynamic modelling are shown in Figure 5 which presents isopleths for M2, H13, P58 and 316L. 316L Stainless steel was modelled as a quinary Fe-Cr-Ni-2.5Mo-2Mn system since the very low carbon content of this alloy (0.03%) would not have a great effect on the solidification range. Mo and Mn were included so that their ferrite and austenite stabilising effects are considered. Isopleths were calculated for Fe-17Cr-Ni-2.5Mo-2Mn and Fe-Cr-12Ni-2.5Mo-2Mn. These are given in Figures 5(a) and (b), respectively. At the 316L composition (Fe-17Cr-12Ni-2.5Mo-2Mn) the solidus-liquidus interval is narrow, ~5°C. This is consistent with what could be inferred from the experimental determined data for the Fe-Cr, Cr-Ni, Ni-Fe binary and Fe-Ni-Cr ternary systems presented by Raynor and Rivilin, [15].

Table 3: Assessment of the processability of various alloy systems (gas atomised powders)

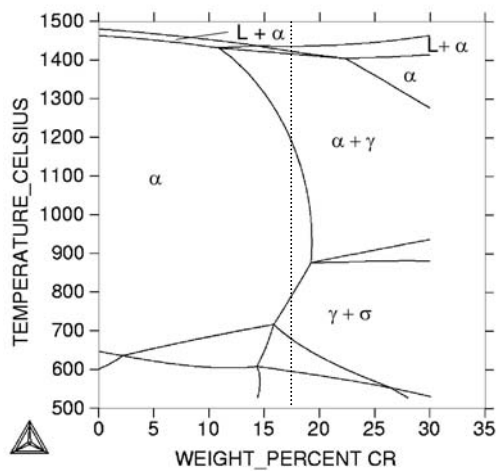| Alloy	Nominal Composition	Laser System	Density	Processability	$T_L - T_s$ (^{o}C)	Ref
316L	Fe - 12Ni - 17Cr - 2.5Mo-2Mn - 0.03C	Nd-Yag	99-100%	v.good	5	[3]
H13	Fe – 5Cr – 1.5Mo – 1V – 1Si – 0.4C	Nd-Yag CW-CO2	~90%	good	110	[12]
H13+0.4C	Fe-5Cr-1.5Mo-1V-1Si-0.8C	Nd-Yag	62%	poor	180	[12]
H13+0.8C	Fe-5Cr-1.5Mo-1V-1Si-1.2C	Nd-Yag	60%	poor	200	[12]
M2	Fe – 6Mo – 5W-4Cr – 2V – 0.8C	Nd-Yag CW-CO2	67%	poor	200	[10]
P58	Fe – 14Mo – 4Cr – 1.4C	CW-CO2	~70%	poor	170	[9]

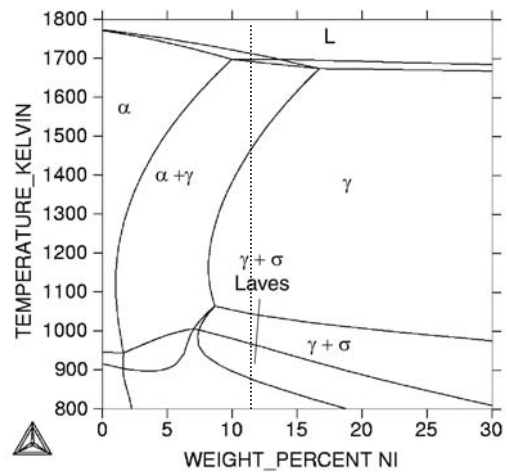Fig 5a. Isopleth through the Fe-Cr-Ni-2Mn-2.5Mo system at 17Cr. 316L

Fig

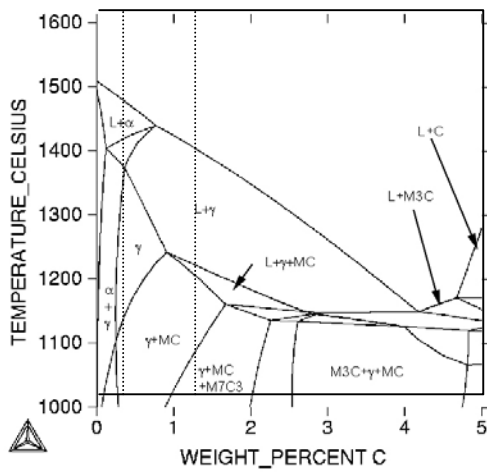Fig 5b Isopleth through the Fe-Cr-Ni-2Mn-2.5Mo system at 12Ni. 316L

Figure 5c Isopleth for the Fe-C-5Cr-1.5Mo-1V-1Si system. (H13)
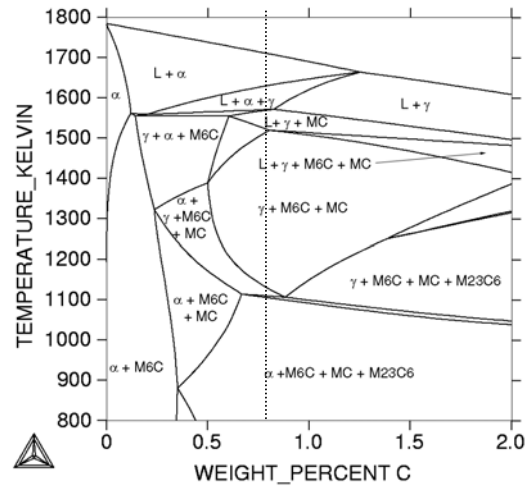

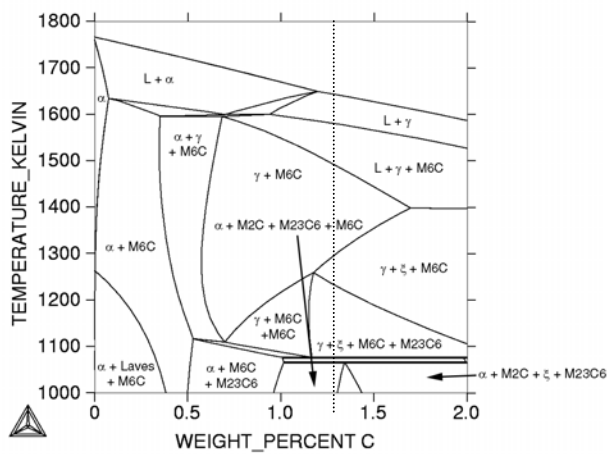Figure 5d Isopleth for the Fe-6W-5Mo-4Cr-2V-C system after suspending the WC phase.(M2)

Figure 5e. Isopleth for Fe – 14Mo – 4Cr – C calculated. P58

Figure 5.   Calculated Isopleths for M2, P58, 316L and H13.

148

For processing under comparable scan conditions, alloys with short melting / freezing ranges, e.g. 316L where $T_{Liquidus} - T_{Solidus} = \sim5^{o}C$, densities up to 99% can be obtained [3] whilst long melting / freezing range alloys such as M2 ($T_L - T_S = \sim200^{o}C$) could only be processed to densities of only ~65-70% [7]. For H13 $T_L - T_S = \sim110^{o}C$ and maximum density achieved is ~90%. This correlates with the degradation in processability noted for H13 powder with increasing carbon content [12]. Thus, there would appear to be a direct correlation between alloy solidification range and powder processability. Increasing solidification range corresponds to a significant decrease in ease of processing. Hence this would imply that one of the important factors in determining a good build is melt fluidity with high fluidity being a desirable property. Verification of this would be achieved by processing pre-alloyed powders prepared from short freezing range alloys, i.e. eutectic or near eutectic compositions.

Conclusions
Prealloyed H13 die steel powders are more amenable to processing via DLMR than M2 high speed steel powders

There is a correlation between processibility (resultant density and surface finish) and freezing range for high alloy steel powders processed by DMLR. A short freezing correlates to good processibility.

References
[1]   KW Dalgarno & CS Wright; "Approaches to Processing Metal and Ceramics through the Laser Scanning of Powder Beds", *Society of Manufacturing Engineers,* Technical Paper PE03-143, 2003.
[2]   C Hauser, THC Childs & KW Dalgarno, "Selective Laser Sintering of Stainless Steel 314HC Processed Using Room Temperature Powder Beds", proc. *Solid Freeform Fabrication Symposium* Austin, Texas August 9 – 11, 1999, pp273-280.
[3]   RH Morgan AJ Papworth, C Sutcliffe, P Fox & W O'Neill, "High Density Net Shape Components by Direct Laser Re-melting of Single Phase Powders", *J Materials Science*, 2002, **37**, 3093-3100.
[4]   NJ Niu & ITH Chang, "Selective Laser Sintering of Gas and Water Atomised High Speed Steel Powders", *Scripta Materialia,* 1999, **41**, pp 25 – 30.
[5]   NJ Niu & ITH Chang, "Instability of Scan Tracks of Selective Laser Sintering of High Speed Steel Powder", *Scripta Materialia,* 1999, **41**, pp 1229 – 1234.
[6]   MM Dewidar, "Direct and Indirect Laser Sintering of Metals" *PhD Thesis*, University of Leeds, 2002.
[7]   SP Akhtar et.al, Proc.of EuroPM2003, Vol 3, pp379-384, Shrewsbury, EPMA, 2003.
[8]   C Hauser, "Selective Laser Sintering of stainless steel powder", *PhD Thesis,* University of Leeds, 2003.
[9]   MM. Dewider, KW Dalgarno & CS Wright, *Proc I. Mech.E,* 2003, **217,**Part B, 1651-1663

[10] SP Akhtar *et.al*. proc. "Direct Selective Laser Sintering of Tool Steel Powders to High Density: Part B – The Effect on Microstructural Evolution", Proc *14th Solid Freeform Fabrication Symposium* Austin, Texas August 4 – 6, 2003

[11] G Hoyle, "Modification of the Cast Structure of High Speed Steel", *J.Iron Steel Institute,* 1959, November, pp254-269.

[12] JW Xie, Proc of EuroPM2003, Vol 3, pp473-478, Shrewsbury, EPMA, 2003.

[13] C. Hauser , to be presented at Proc *15th Solid Freeform Fabrication Symposium* Austin, Texas August 2 – 4, 2004

[14] CS Wright & SP Akhtar, to be presented at EuroPM2004, October 2004.

[15] G V Raynor and V G Rivlin: Phase Equilibria in Iron Ternary Alloys, Institute of Metals, 1988.

[16] R.M.German " A quantitative theory for supersolidus liquid phase sintering" Powder Metallurgy, Vol 34 (2), pp101-107, 1991.

[17] C.S.Wright. M Youseffi, A.S.Wronski, I.Ansara, M. Durand-Charre, Y.Bienvenu, F. Lemoisson, J.M.G. Mascarenhas and M.M. Oliveira: "Supersolidus liquid phase sintering of high speed steels-Part 3 the computer aided design of sinterable alloys." Powder Metallurgy, Vol 42, Issue 2, ppl-16, 1999.

[18] J. Campbell: "Castings" Butterworth-Heinemann, 1991.